ChemPubSoc Europe

DOI: 10.1002/cmdc.201500420

CHEMMEDCHEM Full Papers

^{11}C- and ^{18}F-Labeled Radioligands for P-Glycoprotein Imaging by Positron Emission Tomography

Mariangela Cantore,*[a, b] Marcel Benadiba,[a] Philip H. Elsinga,[a] Chantal Kwizera,[a] Rudi A. J. O. Dierckx,[a] Nicola Antonio Colabufo,[b, c] and Gert Luurtsema[a]

P-Glycoprotein (P-gp) is an efflux transporter widely expressed at the human blood–brain barrier. It is involved in xenobiotics efflux and in onset and progression of neurodegenerative disorders. For these reasons, there is great interest in the assessment of P-gp expression and function by noninvasive techniques such as positron emission tomography (PET). Three radiolabeled aryloxazole derivatives: 2-[2-(2-methyl-(^{11}C)-5-methoxyphenyl)oxazol-4-ylmethyl]-6,7-dimethoxy-1,2,3,4-tetrahydroisoquinoline ([^{11}C]-**5**); 2-[2-(2-fluoromethyl-(^{18}F)-5-methoxyphenyl)oxazol-4-ylmethyl]-6,7-dimethoxy-1,2,3,4-tetrahydroisoquinoline ([^{18}F]-**6**); and 2-[2-(2-fluoroethyl-(^{18}F)-5-methoxyphenyl)oxazol-4-ylmethyl]-6,7-dimethoxy-1,2,3,4-tetrahydroisoquinoline ([^{18}F]-**7**), were tested in several in vitro biological assays to assess the effect of the aryl substituent in terms of potency and mechanism of action toward P-gp. Methyl derivative [^{11}C]-**5** is a potent P-gp substrate, whereas the corresponding fluoroethyl derivative [^{18}F]-**7** is a P-gp inhibitor. Fluoromethyl compound [^{18}F]-**6** is classified as a non-transported P-gp substrate, because its efflux increases after cyclosporine A modulation. These studies revealed a promising substrate and inhibitor, [^{11}C]-**5** and [^{18}F]-**7**, respectively, for in vivo imaging of P-gp by using PET.

Introduction

P-Glycoprotein (P-gp, ABCB1) is the best-known and most-studied ATP binding cassette (ABC) transporter.[1] This protein is widely expressed in barriers and excretory tissues, in which it modulates the entry of a broad range of structurally unrelated compounds by active ATP-driven efflux transport. P-gp is highly expressed on the luminal membrane of the endothelial cells at the blood–brain barrier.[2] Owing to this crucial localization, it plays an important role in maintaining homeostasis in the central nervous system by protecting the brain from accumulation of toxic compounds by extruding them from the brain into the blood.

Recently, scientific evidence demonstrated that changes in P-gp function and/or expression are involved in the onset and progression of neurodegenerative diseases such as Alzheimer's disease and Parkinson's disease.[3–5] Many studies have demonstrated that P-gp and other ABC transporters such as breast cancer resistance protein (BCRP) and multidrug resistance associated protein 1 (MRP1) play a pivotal role in controlling β-amyloid peptide levels in the brain to avoid formation of amyloid plaques, the major hallmark of Alzheimer's disease.[6] For these reasons, there is great interest in the assessment of P-gp expression and function by noninvasive techniques such as positron emission tomography (PET).

Radiolabeled P-gp substrates such as (*R*)-[^{11}C]verapamil ([^{11}C]-**1**)[7,8] and [^{11}C]-*N*-desmethylloperamide[9] have been used to assess P-gp functional activity. Several studies have been performed with [^{11}C]-**1** (Figure 1),[9] which is the only tracer so far used in clinical studies. Nevertheless, the low signal-to-noise ratio (i.e., modest increase in brain uptake after P-gp inhibition)[10,11] limits its use.

The presence of radiolabeled metabolites can result in difficulties in quantification of the PET data. Moreover, the low brain uptake of (*R*)-[^{11}C]verapamil ([^{11}C]-**1**) limits its use. Especially, if there is overexpression of P-gp at the blood–brain barrier,[12] the uptake of the tracer will be even lower than that in normal tissue. To overcome these limitations, a strategy to use a selective P-gp inhibitor could be an option. Therefore, several labeled inhibitors have been evaluated for PET imaging of P-gp expression, including [^{11}C]laniquidar, [^{11}C]tariquidar ([^{11}C]-**2**), [^{11}C]elacridar, [^{18}F]fluoroethyltariquidar, [^{18}F]fluoroethylelacridar, and 1-[^{18}F]fluoroelacridar[13] (Figure 1).

However, it was observed that these compounds, which act as inhibitors at pharmacological dose, are at tracer concentrations recognized by P-gp and BCRP as substrates, which results in low brain uptake of the PET probes.[13–15] These findings encourage the search and screening of more specific, novel radiolabeled compounds that could image either P-gp or BCRP transporters.[16–18]

Given that ABC transporters are flexible proteins that bind to several distinct molecules, it is a challenge to find specific

[a] *Dr. M. Cantore, M. Benadiba, P. H. Elsinga, C. Kwizera, R. A. J. O. Dierckx, G. Luurtsema*
Department of Nuclear Medicine and Molecular Imaging
University Medical Center Groningen, University of Groningen
Hanzeplein 1, 9713 GZ Groningen (The Netherlands)
E-mail: mariangelacantore@gmail.com

[b] *Dr. M. Cantore, N. A. Colabufo*
Biofordrug s.r.l., Spin-off dell'Università degli Studi di Bari "A. Moro"
via Orabona 4, 70125, Bari (Italy)
Fax: (+39) 0805442231

[c] *N. A. Colabufo*
Dipartimento di Farmacia-Scienze del Farmaco
Università degli Studi di Bari "A. Moro", via Orabona 4, 70125, Bari (Italy)

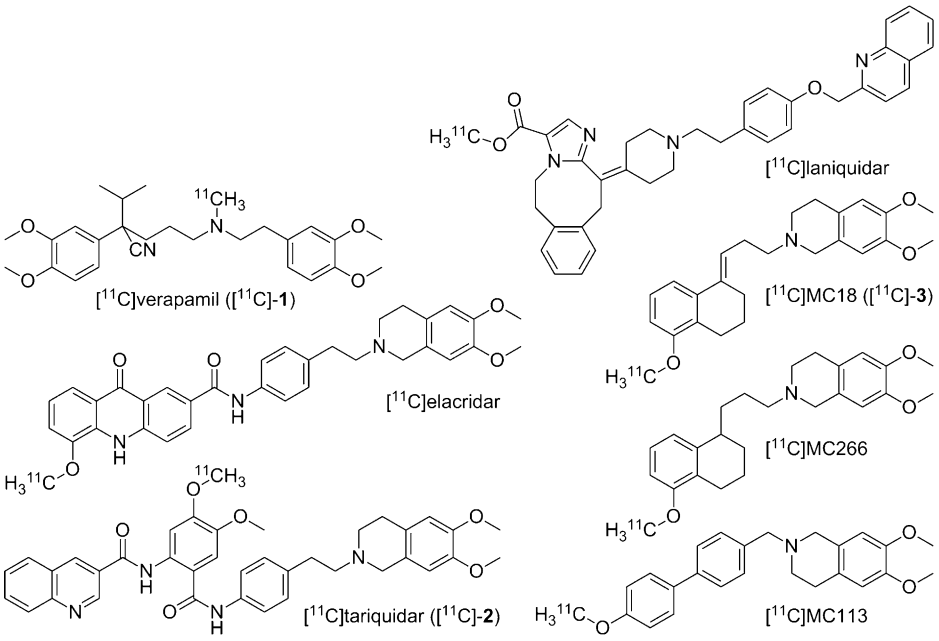

Figure 1. Radiolabeled P-gp/BCRP substrates/inhibitors.

radiolabeled compounds that are capable of measuring a single transporter subtype in vivo. Colabufo and colleagues tested several P-gp modulators that behave as substrates, inhibitors, or even inducers depending on slight changes in their molecular structures.[19–22] In a preclinical study, two new PET probes were developed: a P-gp inhibitor [^{11}C]MC18 ([^{11}C]-**3**), which showed specific binding in the brain and several peripheral target organs and is, therefore, useful to assess P-gp expression, and [^{11}C]MC266 ([^{11}C]-**4**), a P-gp substrate with higher baseline uptake than [^{11}C]-**1** suitable for measurement of P-gp activity.[18] In a recent PET study, the new compound [^{11}C]MC113 was tested in mice.[17] However, although this tracer showed a higher target organ uptake than [^{11}C]-**4**, it failed to provide a P-gp-specific signal both at the mouse blood–brain barrier and in a tumor model. Probably, the tracer has insufficient binding affinity to P-gp.

On the basis of Polli's classification,[23] it is possible to discriminate between P-gp inhibitors, substrates, and substrate modulators.[21] Therefore, we determined the apparent permeability (P_{app}) for each developed compound in the Caco-2 cell line. In this model system, the basolateral-to-apical (B→A) and apical-to-basolateral (A→B) fluxes for each ligand were evaluated. The B→A flux represents the contribution of passive diffusion, whereas the A→B flux represents P-gp-mediated active transport. The B→A/A→B ratio is useful to distinguish transported drugs from compounds that are not transported. Compounds displaying B→A/A→B >2 are considered P-gp substrates, whereas drugs showing B→A/A→B <2 are not transported by P-gp. Compounds that were not transported by P-gp did not deplete ATP in this cell line, whereas compounds transported by P-gp depleted ATP in a dose- and time-dependent manner. These assays can discriminate between a P-gp inhibitor and a P-gp substrate.[21,23]

The potency (EC_{50}) of each P-gp-modulating agent was determined in Madin–Darby canine kidney cells, stably transfected for P-gp expression (MDCK-MDR1). The selectivity toward other ABC transporters could be evaluated in the same cell line overexpressing either MRP1 (MDCK-MRP1) or BCRP (MDCK-BCRP). This stepwise investigation (i.e., B→A/A→B ratio → ATP depletion → affinity for P-gp → selectivity for P-gp) represents a suitable screening of P-gp candidates for radiolabeling.

On the basis of our previous studies, a new class of compounds, cycloisosteres of MC113, was developed.[24] MC150 (**5**) and the corresponding fluoromethyl and fluoroethyl derivatives (i.e., MC236, **6**, and MC211, **7**) were selected as potential tracers suitable for ^{11}C and ^{18}F labeling. The insertion of a fluoroalkyl moiety can change the biological and metabolic profile of a compound. It is known that slight changes can lead to different P-gp activities. The effect of structural changes of the labeled alkyl moieties of these tracers was evaluated by in vitro assays. The mechanism of interaction of each compound with P-gp and its metabolic profile were determined. In the present study, the radiosynthesis and in vitro evaluation of [^{11}C]-**5**, [^{18}F]-**6**, and [^{18}F]-**7** are presented: our purpose was the development of novel tracers for imaging P-gp activity and expression.

Results and Discussion

Compounds **5** and **7** presented in this work were synthesized in good yields (40–50%), whereas compound **6** was synthesized in low yield (less than 5%) as a result of difficulties in inserting the small fluoromethyl chain. For this reason, compound **6** was chemically characterized but not tested in vitro (Scheme 1).

Compounds [^{11}C]-**5**, [^{18}F]-**7**, and [^{18}F]-**6** (Scheme 2) were prepared in good radiochemical yields, >40% yield for [^{11}C]-**5** and

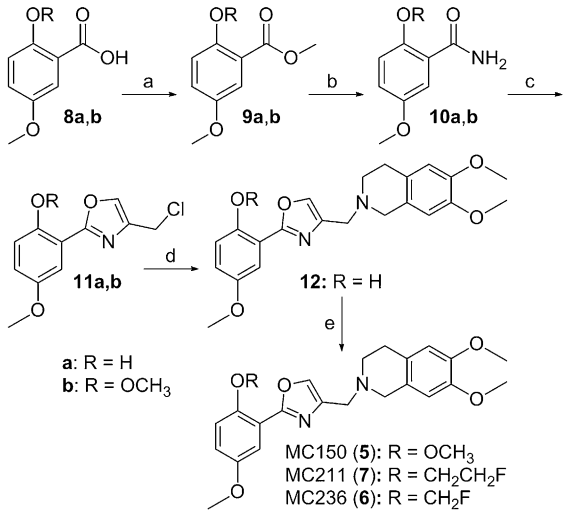

Scheme 1. Synthesis of MC150 (**5**), MC211 (**7**), MC236 (**6**), and precursor **12**. *Reagents and conditions*: a) MeI, Cs_2CO_3, DMF, 30 min, RT (46%); b) 7 N NH_4OH/MeOH, 60 °C, 6 h (90%); c) 1,3-dichloroacetone, 150 °C, 5 h (54%); d) 6,7-dimethoxy-1,2,3,4-tetrahydroisoquinoline, Na_2CO_3, DMF, 150 °C, overnight (82%); e) NaH, DMF, fluoromethyl tosylate or fluoroethyl tosylate, 150 °C, 24 h (2% for **6**, 38% for **7**).

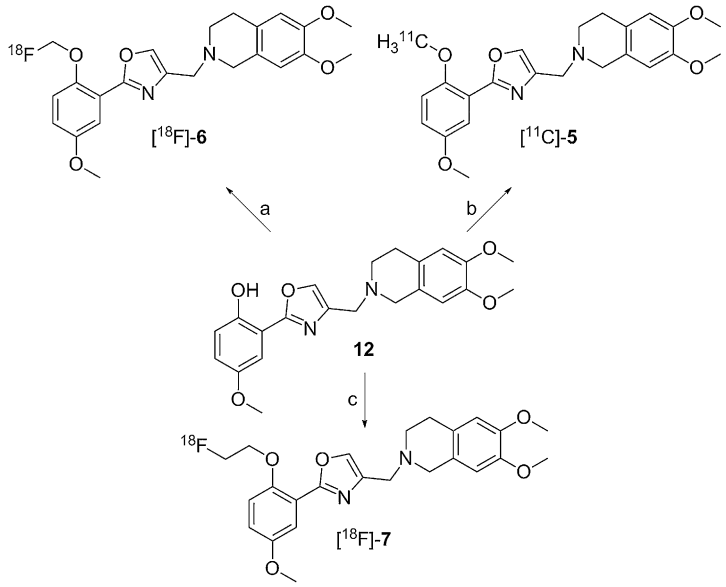

Scheme 2. Radiosynthesis of [^{11}C]-**5**, [^{18}F]-**6**, and [^{18}F]-**7**. *Reagents and conditions*: a) $^{18}FCH_2OTf$, NaH, DMF, 10 min, 125 °C (3–10%); b) $^{11}CH_3I$, DMSO, KOH, 125 °C, 1 min (40%); c) $^{18}FCH_2CH_2OTs$, NaH, DMF, 15 min, 125 °C (3–10%).

3–10% yield for [^{18}F]-**7** and [^{18}F]-**6**, with high specific activity (> 50–100 GBq μmol^{-1}). For the preparation of [^{11}C]-**5**, the use of [^{11}C]CH_3I as a methylating agent led to a successful synthesis, whereas for [^{18}F]-**6**, the [^{18}F]fluorobromomethane synthetic route was not reliable and was characterized by a low yield.

Compounds **5** and **7** were tested for their metabolic stability in human liver microsomes in combination with UPLC–MS-QTOF (ultraperformance liquid chromatography quadrupole time-of-flight mass spectrometry). The metabolic profile of each compound was monitored for 2 h and was evaluated at different time points. Both compounds were stable during this interval. After 120 min of microsomes incubation with **5**, 53% of the total mass still represented parent compound, and the contribution of O-demethylation metabolites was 15%. Demethylation reactions occur within 15 min. In a metabolic study with compound **1**, 45% parent remained after 30 min, together with 11% of demethylation products. In contrast, **5** and **7** showed higher metabolic stability than compound **1**. After 120 min of microsomial incubation with **5**, 53% of the parent remained, with 15% O-demethylated metabolites. For compound **7**, 57% of the parent compound remained after 120 min, together with 15, 12, and 3% products of oxidative defluorination, demethylation, and F-dealkylation, respectively (Figure 2). Loss of the fluoroethyl moiety started after 45 min. For both compounds, cleavage of an N–C bond caused formation of 6,7-dimethoxy-1,2,3,4-tetrahydroisoquinoline, which was identified by MS as a primary metabolite. Metabolic studies in microsomes provide additional information about the stability of the moiety suitable to labeling in candidates radioligands. These findings indicate that from a metabolic point of view, **5** and **7** might be better PET radiotracers candidates than compound **1**.

Compounds **5** and **7** were investigated for their mechanism of interaction with P-gp and their selectivity toward the other efflux pumps MRP1 and BCRP.[24] Because of the low stability of the fluoromethyl moiety under the standard experimental conditions, in in vitro biological assays, compound [^{18}F]-**6** was only investigated in the following functional assays: 1) apparent permeability determination (P_{app}) in Caco-2 cell monolayer; 2) inhibitory activity of the acetoxymethyl esters of calcein-AM transport in MDCK cells overexpressing each transporter (i.e., MDCK-MDR1, MDCK-BCRP, MDCK-MRP1); 3) ATP depletion in MDCK cells. For compound **5**, the transport ratio through Caco-2 monolayers in the basolateral→apical and apical→basolateral directions (P_{app} B→A A^{-1}→B) was 10, and the compound did not activate ATPase activity within the monolayer. Compound **5** showed moderate activity toward P-gp (EC_{50} = 3.1 μM) and BCRP (EC_{50} = 2 μM) in the calcein-AM assay and very low activity toward MRP1 (EC_{50} > 50 μM). For compound **7**, the transport ratio through Caco-2 monolayers in the basolateral→apical and apical→basolateral directions (P_{app} B→A/A→B) was 2.8, and the compound did not activate ATPase activity within the monolayer. Compound **7** showed high affinity for P-gp (EC_{50} = 0.8 μM) and very low activity toward BCRP in the calcein-AM assay (EC_{50} > 50 μM), and it was inactive toward MRP1 (EC_{50} > 100 μM). On the basis of these data, compound **5** was classified, taking into account the classification reported by Polli et al.,[23] as a dual P-gp/BCRP-transported substrate, and compound **7** could be estimated as a selective P-gp inhibitor, although its B→A/A→B ratio is borderline for substrate/inhibitor activity.

All radioligands were evaluated in the P-gp-overexpressing cell line Colo320. After separation of subcellular fractions, the

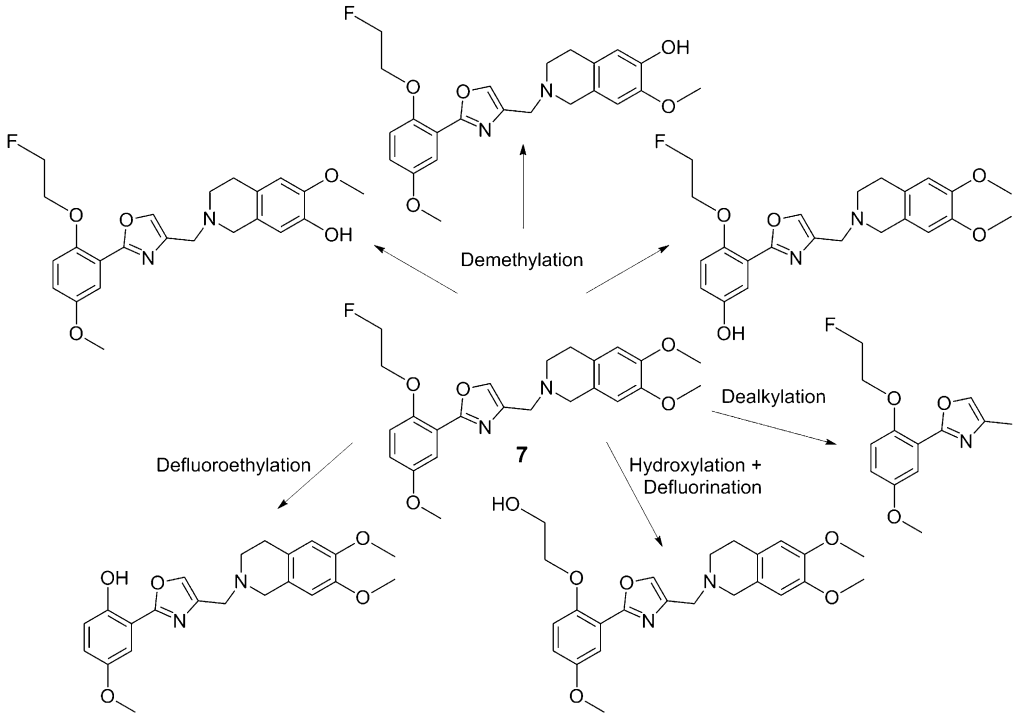

Figure 2. Metabolic pathways for compound **7** in human liver microsomes.

uptake/binding of each tracer in each specific fraction was determined. It is known that P-gp can also be highly expressed in the membranes of vesicles that are located in the cytoplasm.

A very low cellular accumulation of [^{11}C]-**5** and [^{18}F]-**6** was found, significantly lower than that of [^{18}F]-**7** (Figure 3 a, b). These data demonstrate that [^{11}C]-**5** and [^{18}F]-**6** are potent P-gp substrates showing strong efflux. In contrast, [^{18}F]-**7** showed more specific binding to P-gp in both the cytoplasmic and membrane fractions (Figure 3 b).

To confirm or refute that these compounds are selectively transported or effluxed by P-gp, a fractionation experiment was performed in the breast cancer cell line MDA-MB-231, which does not express P-gp but has overexpression of BCRP (Figure 4 a, b).[25] The results demonstrate that [^{18}F]-**7** is significantly less accumulated in the cytoplasmic fraction (Figure 4 a) and more accumulated in the membrane fraction (Figure 4 b) of this cell line relative to [^{11}C]-**5**, which is transported by BCRP. This is in agreement with the previous results that show that **5** is a potent substrate for both P-gp and BCRP, whereas **7** is a compound with high affinity for P-gp and is thought to be an inhibitor. Interestingly, the results demonstrate that [^{18}F]-**7** shows significant binding even if only a very tiny amount of the P-gp transporter is present (see the percentage of injected dose in Figure 3 and compare this with Figure 4 relating to MDA-MB). Thus, in cells that do not express a high amount of P-gp, more cytoplasmic accumulation of the high-affinity substrate [^{11}C]-**5** might be found.

In the transwell permeability assay, the transport of each tracer in Colo320 cells was evaluated. In accordance with the results mentioned above, we found that all radiolabeled compounds were effluxed to the apical side; however, [^{18}F]-**7** was less transported (Figure 5 a). Interestingly, after pretreatment with P-gp modulators **1** and **13** and P-gp inhibitor **3** (Fig-

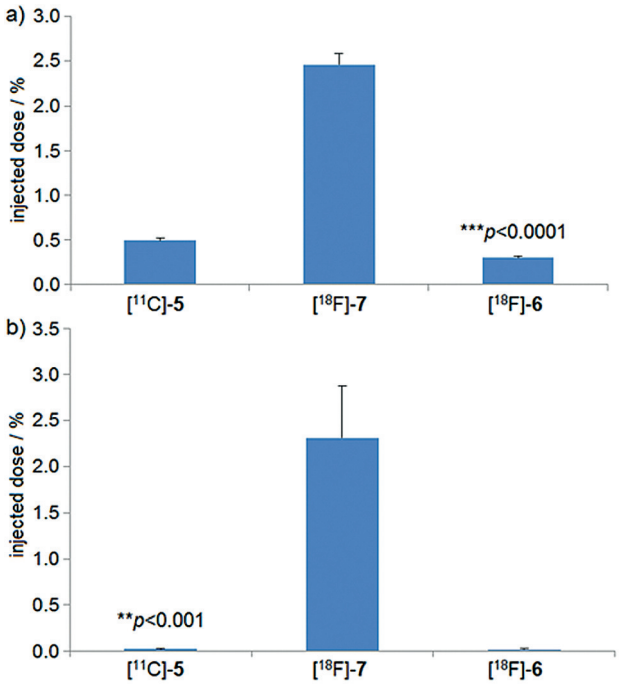

Figure 3. a) Cytoplasmic and b) membrane accumulation of [^{11}C]-**5**, [^{18}F]-**7**, and [^{18}F]-**6** in the P-gp-overexpressing Colo320 cell line. Note that [^{18}F]-**7** is less transported or effluxed outside the cells with a more specific binding to P-gp in both cytoplasmic and membrane fractions. Data are the mean ± SEM, $n = 6$. Student t-test was performed; $p < 0.05$ was considered statistically significant.

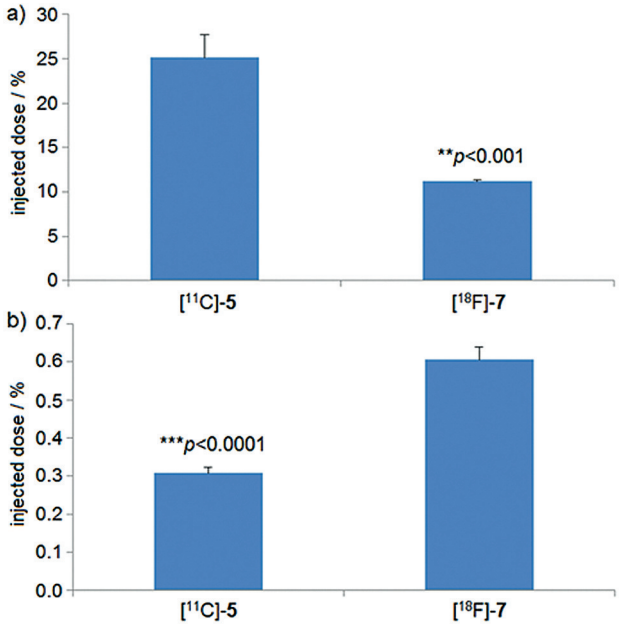

Figure 4. a) Cytoplasmic and b) membrane accumulation of [^{11}C]-**5** and [^{18}F]-**7** in the MDA-MB breast cancer cell line. Data are the mean ± SEM, $n = 6$. Student *t*-test was performed; $p < 0.05$ was considered statistically significant.

ure 5 b), it was found that only inhibitor **3** significantly increased [^{18}F]-**7** permeation to the basolateral side. In contrast, all modulators increased the permeation of [^{11}C]-**5** approximately sixfold (Figure 5 c). Compound [^{18}F]-**6** presented a different profile, as pretreatment with compound **1** increased its permeation 35-fold and pretreatment with compound **3** increased it only 1.3-fold, whereas pretreatment with **13** increased its efflux significantly. This discrepancy could be explained by the assumption that there are many constitutive transport proteins in cells that could bind [^{18}F]-**6** efficaciously if P-gp is modulated. Unfortunately, as reported above, unlabeled **6** is not available, and therefore, additional investigations concerning its specificity could not be performed. Compound [^{11}C]-**1** was also tested in this experiment (Figure 5 e). It was transported more than [^{11}C]-**5**, but its permeation was increased only 5-fold by **3** and only 3.5-fold by **13**. For all the compounds, increased permeation after modulator pretreatment could be attributed to competition between the compounds and the modulators for the same binding site.

An additional experiment with [^{11}C]-**1** as a positive control was performed (Figure 6). In accordance with our speculation, no competition was observed between P-gp modulators **1** and **13** and radiolabeled compound [^{18}F]-**7**. However, both modulators interacted with [^{11}C]-**5** and [^{11}C]-**1** (Figure 6). This interaction suggests that [^{11}C]-**5** binds to the same binding site as **1** and **13**. In contrast, [^{18}F]-**7** accumulated more in both fractions, which suggests that this radiotracer could dislocate the P-gp modulators or bind to a different site on the P-gp molecule. Anyway, [^{18}F]-**7** seems to have greater affinity for P-gp and, therefore, presented a strong and noncompetitive binding property, as it is highly accumulated in the cytosol and in the membrane fractions (Figure 6 a, b) even if pretreated with P-gp modulator **1** or **13**. Ligands **1** and **13** competed with [^{18}F]-**6** in both fractions, although **13** is reported to be a P-gp modulator rather than a P-gp substrate. In addition, as the nonradioactive drugs are added 30 min before the radiotracer, it is also possible that [^{11}C]-**5** and [^{18}F]-**6** cannot displace ligands if they are already attached to the same binding site of the P-gp molecule (resulting in less accumulation of the radiotracer). Interestingly, previously characterized P-gp inhibitor **3**[26] increased the permeation of all radiolabeled compounds to the basal side. However, for inhibitor [^{18}F]-**7** we can conclude that increased permeation to the basal side is due to

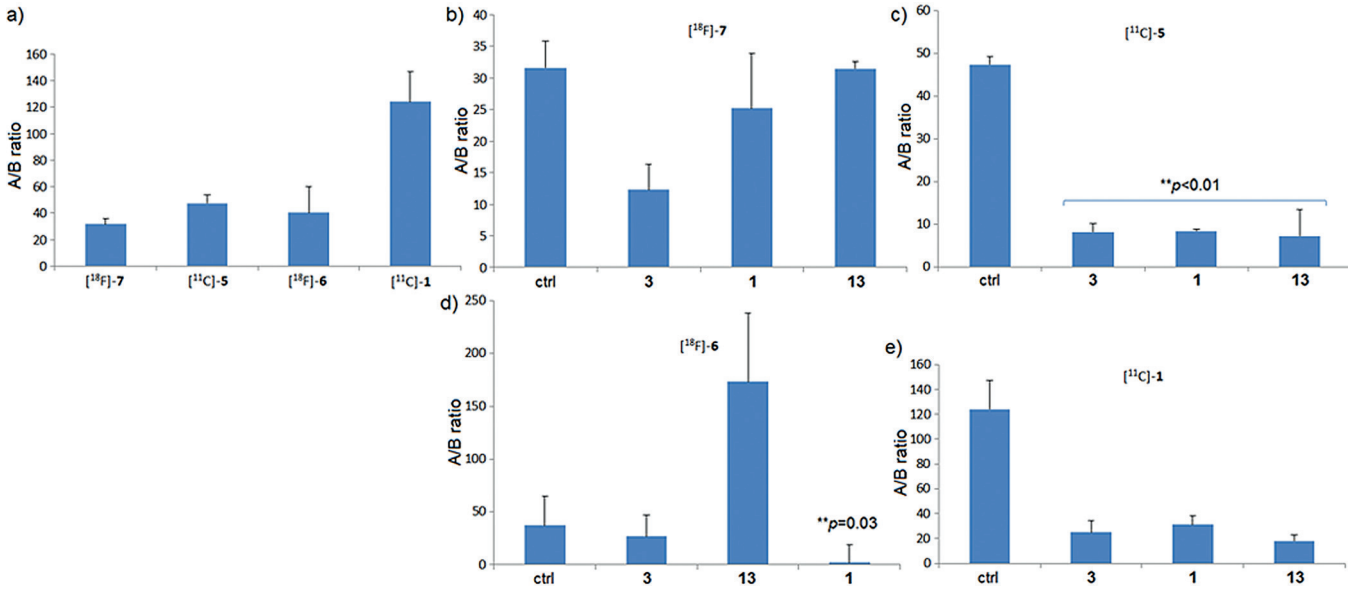

Figure 5. a) Transwell permeability assay in the Colo320 cell line showing a higher transport activity of [^{11}C]-**5** to the apical side than the inhibitor [^{18}F]-**7**. Transwell permeability assays in the Colo320 cell line after pretreatment with MC18 (**3**), verapamil (**1**), and cyclosporine A (**13**) for b) [^{18}F]-**7**, c) [^{11}C]-**5**, d) [^{18}F]-**6**, and e) [^{11}C]-**1**. A/B: apical/basolateral ratio; data are the mean ± SEM, $n = 3$.

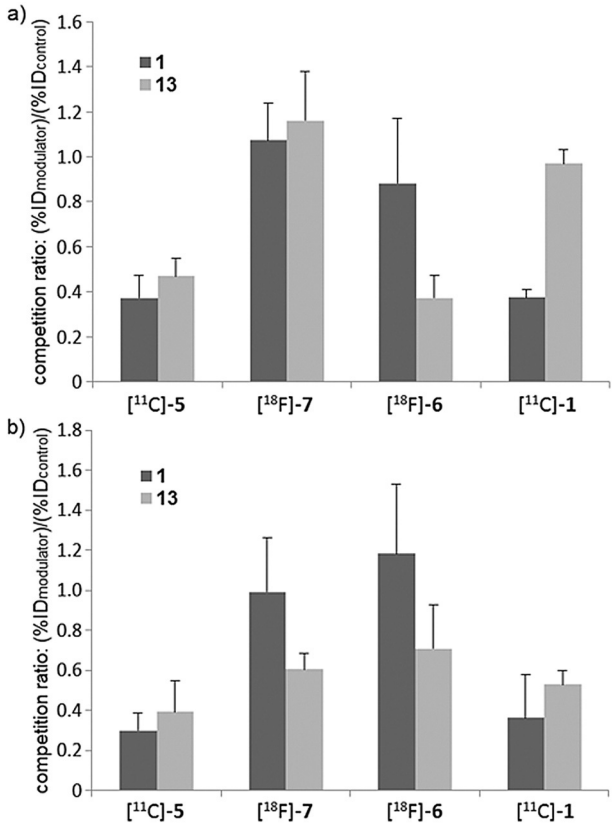

Figure 6. Competition assay in the Colo320 cell line for [^{18}F]-**7**, [^{11}C]-**5**, [^{18}F]-**6**, and [^{11}C]-**1**. a) Cytoplasmic and b) membrane fraction obtained from the P-gp-overexpressing cell line Colo320 after pretreatment with P-gp modulators **1** (dark grey) and **13** (light grey). Data are corrected for the values obtained from the controls. %ID: percentage of the injected dose. Data are the mean ± SEM, $n = 6$. Student *t*-test was performed; $p < 0.05$ was considered statistically significant.

a competition between tracer and inhibitor drug for the same binding site. This result also confirmed our previous hypothesis suggesting that the P-gp modulators verapamil and cyclosporin bind to a site different from the binding site of [^{18}F]-**7** (Figure 6b).

In summary, methyl derivative [^{11}C]-**5** represents a new metabolically stable P-gp/BCRP substrate, whereas insertion of a fluoroethyl moiety instead of a methyl group results in [^{18}F]-**7**, a P-gp inhibitor. Insertion of a fluoromethyl moiety instead of a fluoroethyl group leads to compound [^{18}F]-**6**, which shows a different profile: it binds to the same site as **1**, but in the presence of inhibitor **3**, its permeation increases a few fold, whereas in the presence of **13** its efflux increases.

Conclusions

In this work, three new compounds, 2-[2-(2-methyl-(^{11}C)-5-methoxyphenyl) oxazol-4-ylmethyl]-6,7-dimethoxy-1,2,3,4-tetrahydroisoquinoline ([^{11}C]-**5**), 2-[2-(2-fluoromethyl-(^{18}F)-5-methoxyphenyl)oxazol-4-ylmethyl]-6,7-dimethoxy-1,2,3,4-tetra-hydroisoquinoline ([^{18}F]-**6**), and 2-[2-(2-fluoroethyl-(^{18}F)-5-methoxyphenyl)oxazol-4-ylmethyl]-6,7-dimethoxy-1,2,3,4-tetrahydroisoquinoline ([^{18}F]-**7**), were presented. All were synthesized with high specific activity and in acceptable radiochemical yields. The preliminary in vitro results of cold compounds were confirmed at the tracer level, which confirms that small changes in the molecular structures could lead to different P-gp and BCRP activities. These data can lead to better understanding of the main structural requirements for the development of novel P-gp tracers. Compound [^{11}C]-**5** represents a new substrate, with P-gp activity similar to that of (*R*)-[^{11}C]verapamil ([^{11}C]-**1**) and improved metabolic stability. However, with respect to [^{11}C]-**1**, ligand [^{11}C]-**5** is more sensitive in terms of cell uptake in the presence of inhibitor and modulator than verapamil, and this aspect is important because cell radiotracer accumulation is employed to quantify P-gp activity. On the other hand, [^{18}F]-**7** represents a new P-gp inhibitor. For [^{18}F]-**6**, it is important to determine its mechanism of interaction with P-gp, although several pharmacokinetic limitations discourage these additional studies.

Experimental Section

General procedures

Column chromatography was performed with 1:30 Merck silica gel 60 A° (63–200 μm) as the stationary phase. Melting points were determined in open capillaries with a Gallenkamp electrothermal apparatus. ^{1}H NMR spectra were recorded in $CDCl_3$ at 300 MHz with a Varian Mercury-VX spectrometer. All spectra were recorded on the free bases. All chemical shift values are reported in ppm (δ). Recording of mass spectra was done with an HP6890–5973 MSD gas chromatograph/mass spectrometer; only significant *m/z* peaks, with their percentages of relative intensity in parentheses, are reported. All spectra were in accordance with the assigned structures. ESI-MS analyses were performed with an Agilent 1100 LC–MS Dtrap system VL. Purity of final compounds was established by combustion analysis of the corresponding hydrochloride salts, which confirmed a purity ≥ 95 %.

For radiolabeled compounds, detection on TLC was performed with Cyclone phosphor storage screens (multisensitive, Packard, PerkinElmer Life and Analytica Science). These screens were exposed to the TLC strips and subsequently read out by using a Cyclone phosphor storage imager (PerkinElmer) and were analyzed with OptiQuant software. Radiolabeled compounds were also identified by analysis by using a Waters UPLC Acquity H class with a BEH-C18 analytical column (2.1 × 50 mm, 1.7 μm). A gradient of 0.1 % formic acid/acetonitrile was used as the mobile phase at a flow rate of 0.6 mL min^{-1} (formic acid from 98 to 2 % in 16 min) and electrospray ionization (ESI$^+$) mass spectra were acquired at unit resolution from *m/z* = 200 to 1200.

HPLC purifications and analysis were performed with an Elite LaChrom VWR Hitachi L-2130 pump system connected to a UV spectrometer (Elite LaChrom VWR Hitachi L-2400 UV detector) set at a wavelength of 260 nm and a radiation detector (Bicron). Semipreparative HPLC was performed by using a Phenomenex Luna C18-column (10 mm × 250 mm, 5 μm), with sodium acetate/acetonitrile (6:4) as the mobile phase at a flow rate of 4 mL min^{-1}. Quality control was performed on a reverse-phase Symmetric Shield-C18 column (4.6 mm × 250 mm, 5 μm) with sodium acetate/acetonitrile (6:4) as the mobile phase at a flow rate of 1 mL min^{-1}.

All products were formulated with the following procedure. The mixture was passed over an Oasis HLB Sep-Pak to remove acetoni-

trile, and the cartridge was washed with water (2×8 mL), and then the product was eluted from the Oasis HLB Sep-Pak with sterile ethanol (1 mL). The formulated product was suitable to perform all in vitro experiments. Radioactivity measurements during cell studies were done by using an automated gamma counter (LKBG-Compugamma CS 1282, Wallac, Waltham, USA).

Materials

Commercially available chemicals were purchased from Sigma–Aldrich. Verapamil was purchased by Sigma–Aldrich; tariquidar was purchased by API Services, Inc.; cyclosporine A (Sandimmune, 50 mg mL^{-1} solution in polyoxyethylated Ricinus oil) was a product of Sandoz, adenosine 5′-triphosphate (ATP) was purchased from Sigma–Aldrich. Stock solutions of 10 mM of these compounds were prepared fresh prior to the experiment. Subcellular fraction buffer was prepared by the combination of the following reagents: 250 mM sucrose, 20 mM HEPES (2-[4-(2-hydroxyethyl)piperazin-1-yl]ethanesulfonic acid; pH 7.4; Life Technologies), 10 mM KCl (Merck), 1.5 mM $MgCl_2$ (Merck), 1 mM EDTA (ethylenediaminetetraacetic acid; Merck), 1 mM EGTA (ethylene glycol tetraacetic acid; Sigma–Aldrich), DTT (dithiothreitol; Sigma–Aldrich), and protease inhibitor cocktail (Sigma–Aldrich).

QMA-light Sep-Pak cartridges were purchased from Waters and were conditioned with 1.4% aq. sodium hydrogen carbonate (5 mL) and water (100 mL) prior to use. Silica Sep-Pak cartridges, Sep-Pak Alumina N cartridge, and Oasis HLB Sep-Pak were purchased from Waters and were used as received without any preconditioning. A silver triflate column was prepared as described previously.[27] The yield of conversion of [^{11}C]CH_3I into [^{11}C]CH_3 triflate was calculated with a radioassay by employing 4-(4-nitrobenzyl)pyridine.[28] The column was heated to 190 °C under He flow (110 mL min^{-1}) before starting the synthesis.

Cell lines

Cell culture reagents were purchased from Celbio s.r.l. (Milan, Italy). CulturePlate 96-well plates were purchased from PerkinElmer Life Science; calcein-AM and MTT (3-[4,5-dimethylthiazol-2-yl]-2,5-diphenyltetrazoliumbromide) were obtained from Sigma–Aldrich (Milan, Italy). MDCK-MDR1, MDCK-BCRP, and MDCK-MRP1 cell lines were a gift of Professor P. Borst, NKI-AVL Institute, Amsterdam, The Netherlands. All MDCK cells were grown in Dulbecco's modified Eagle's medium (DMEM) high glucose supplemented with 10% fetal bovine serum, 2 mM glutamine, 100 U mL^{-1} penicillin, and 100 g mL^{-1} streptomycin in a humidified incubator at 37 °C with a 5% CO_2 atmosphere. Caco-2 cells were a gift of Dr. Aldo Cavallini and Dr. Caterina Messa from the Laboratory of Biochemistry, National Institute for Digestive Diseases, "S. de Bellis", Bari, Italy.

P-gp-overexpressing Colo320 colon carcinoma and the P-gp noninduced MDA-MB breast cancer cell lines were kindly provided by the Medical Oncology Department of the UMCG, and stocks were maintained frozen (liquid nitrogen) in Roswell Park Memorial Institute medium (RPMI) and DMEM respectively, supplemented with 10% fetal calf serum and 10% sodium dodecyl sulfate (SDS). Stock cells were grown in RPMI or DMEM plus 1% glutamine containing 10% fetal calf serum without antibiotics. From a more or less confluent 25 cm^2 flask, cells were harvested by trypsinization (trypsin 0.025%) and then counted by using an improved Neubauer counting chamber. Cells were seeded into 24-well plates at a density of 7×10^4 cells per well and incubated in a humidified atmosphere of 5% CO_2, 95% air at 37 °C. After 48 h, cells in the exponential phase of growth were used. Cells were pre-incubated for 30 min with distinct P-gp modulators together with or without ATP, followed by 30 min tracer incubation.

Synthesis

Nonlabeled chemistry

Compounds **5**, **6**, and **7** and precursor **12** were synthesized as reported in Scheme 1. Compound **5** was synthesized as previously reported, and spectral data were identical to those previously described.[23] Intermediates **10a** and **10b** were prepared by ammonolysis of methyl esters **9a** and **9b**. Amides **10a** and **10b** were cyclized in the presence of 1,3-dichloroacetone to give oxazoles **11a** and **11b**, which were condensed with 6,7-dimethoxy-1,2,3,4-tetrahydroisoquinoline to obtain precursor **12** and **5**. Compound **7** was synthesized from phenol **12** and fluoroethyl tosylate, which was previously prepared by reaction of fluoroethanol and *p*-toluensulfonyl chloride. Compound **6** was prepared from precursor **5** by reaction with fluoromethyl tosylate previously synthesized from bis(tosylate) and silver *p*-toluenesulfonate.

Methyl 2-hydroxy-5-methoxybenzoate (9a): 2-Hydroxy-5-methoxybenzoic acid (**8a**, 1 mmol) was dissolved in DMF (5 mL). Cesium carbonate (0.8 mmol) was added, and the mixture was stirred at 0 °C for 10 min. CH_3I (1.1 mmol) was added dropwise over 5 min, and the mixture was warmed to RT. After 30 min, water (30 mL) was added, and the aqueous layer was extracted with EtOAc (3× 20 mL) and Et_2O (3×20 mL). The combined organic layer was washed with 10% $NaHCO_3$ (50 mL) and a saturated aqueous solution of NaCl (3×30 mL), dried (Na_2SO_4), and concentrated under reduced pressure to give an oily residue. The crude compound was purified by column chromatography ($CHCl_3$/EtOAc = 1:1) to give a brown oil (46%). GC–MS: *m/z* (%): 182 (42) $[M]^+$, 150 (100), 107 (29).

2-Hydroxy-5-methoxybenzamide (10a): Methyl ester **9a** (4 mmol) was dissolved in methanolic ammonia solution (15 mL, 7 N), and the mixture was warmed at 60 °C for 5 h. The solution was cooled and concentrated to dryness. The crude product was purified by column chromatography ($CHCl_3$/EtOAc = 1:1) to give a white solid (90%); mp: 148–149 °C. ^{1}H NMR: δ = 3.79 (s, 3H, CH_3), 5.96 (br, 2H, NH_2, exchange with D_2O), 6.93–7.08 (m, 3H,) 11.59 ppm (br, 1H, OH, exchange with D_2O). GC–MS: *m/z* (%): 167 (37) $[M]^+$, 150 (100), 107 (40), 79 (26).

2-[4-(Chloromethyl)oxazol-2-yl]-4-methoxyphenol (11a): Amide **10a** (1 mmol) was condensed with 1,3-dichloroacetone (2 mmol) with heating at 150 °C for 5 h. After cooling to RT, H_2O (10 mL) and EtOAc (10 mL) were added. The aqueous phase was extracted with EtOAc (3×50 mL), and the combined organic layer was dried (Na_2SO_4) and concentrated. The residue was purified by column chromatography (hexane/EtOAc = 9:1) to give a yellow solid (54%). ^{1}H NMR: δ = 3.82 (s, 3H, CH_3), 4.56 (s, 1H, CH_2), 4.57 (s, 1H, CH_2), 6.98–7.02 (m, 2H), 7.25 (s, 1H), 7.69 (s, 1H), 10.45 ppm (br, 1H, OH, exchange with D_2O); GC–MS: *m/z* (%): 241 (32) $[M+2]^+$, 239 (94) $[M]^+$, 224 (100), 176 (26).

2-[2-(2-Hydroxy-5-methoxyphenyl)oxazol-4-ylmethyl]-6,7-dimethoxy-1,2,3,4-tetrahydroisoquinoline (12): A mixture of 4-chloromethyl-2-aryloxazole **11a** (0.50 mmol), 6,7-dimethoxytetrahydroisoquinoline (1.2 mmol), and Na_2CO_3 (0.50 mmol) in DMF (5 mL) was stirred overnight. The solvent was evaporated, and the crude product was washed with H_2O (2×20 mL) and extracted with $CHCl_3$ (30 mL). The organic layer was dried (Na_2SO_4) and concentrated

under reduced pressure. The crude product was purified by column chromatography ($CHCl_3$/MeOH = 19:1) and recrystallized (MeOH/Et_2O). Yield: 82%. ^{1}H NMR ($CDCl_3$): δ = 2.78–2.81 (m, 4H, NCH_2CH_2), 3.74 (s, 2H, CH_2NCH_2), 3.75 (s, 2H, CH_2NCH_2), 3.81 (s, 3H, CH_3), 3.82 (s, 6H, CH_3), 3.82 (s, 3H, CH_3), 6.59 (s, 1H), 6.51 (s, 1H), 6.96–6.98 (m, 2H), 7.30 (s, 1H), 7.64 (s, 1H), 10.75 ppm (s, br, 1H, OH, exchange with D_2O); MS (ESI$^+$): *m/z*: 419 [*M* + Na]$^+$; MS–MS (ESI$^+$): *m/z* (%): 404 (4), 226 (100); Anal. calcd for $C_{22}H_{24}N_2O_5HCl{\cdot}0.5\,H_2O$: C 66.65, H 6.10, N 7.07, found: C 66.15, H 6.02, N 6.98.

2-Fluoroethyltosylate: A solution of 2-fluoroethanol (2 mmol) and *p*-toluenesulfonyl chloride (1.1 mmol) in 5 M NaOH (1.6 mmol) was stirred at RT for 24 h. The mixture was diluted with CH_2Cl_2, and the organic phase was washed with 10% NaOH. The organic layer was dried (Na_2SO_4) and concentrated under reduced pressure. The crude product was purified by column chromatography (CH_2Cl_2) to give a colorless oil (92%). ^{1}H NMR: δ = 2.45 (s, 3H, CH_3), 4.21 (t, 1H, CH_2), 4.30 (t, 1H, CH_2), 4.49 (t, 1H, CH_2), 4.64 (t, 1H, CH_2), 7.34 (d, *J* = 8 Hz, 2H), 7.80 ppm (d, *J* = 8 Hz, 2H); MS (ESI$^+$): *m/z*: 241 [*M* + Na]$^+$; MS–MS (ESI+): *m/z* (%): 241 (74), 97 (100).

2-[2-(2-Fluoroethyl-5-methoxyphenyl)oxazol-4-ylmethyl]-6,7-dimethoxy-1,2,3,4-tetrahydroisoquinoline (7): A suspension of NaH (60%, 1.2 mmol) in dry DMF (3 mL) was stirred at RT for 10 min. A solution of phenol **3a** (1 mmol) in DMF (1 mL) was added, and the solution was stirred for 1 h. A solution of 2-fluoroethyl tosylate (1.1 mmol) in DMF (1 mL) was added, and the mixture was stirred for 4 h. Water was added until effervescence ceased. The solvent was evaporated, and the residue was partitioned between H_2O (20 mL) and $CHCl_3$ (20 mL). The organic phase was separated, and the aqueous phase was extracted with $CHCl_3$ (3 × 50 mL). The combined organic fraction was dried (Na_2SO_4) and concentrated. The residue was purified by column chromatography ($CHCl_3$/MeOH = 19:1) and recrystallized (MeOH/Et_2O). Yield: 38%. ^{1}H NMR: δ = 2.88–3.19 (m, 4H, NCH_2CH_2), 3.80–3.98 (m, 4H, CH_2NCH_2), 3.81 (s, 3H, CH_3), 3.83 (s, 3H, CH_3), 3.84 (s, 3H, CH_3), 4.21–4.33 (m, 2H, CH_2CH_2F), 4.68–4.86 (m, 2H, CH_2CH_2F), 6.52 (s, 1H), 6.60 (s, 1H), 6.97–6.98 (m, 2H), 7.49 (s, 1H), 8.02 ppm (s, 1H); MS (ESI$^+$): *m/z:* 443 [*M* + H]$^+$; MS–MS (ESI$^+$): *m/z* (%): 250 (100), 222 (44), 195 (47), 149 (13); Anal. calcd for $C_{24}H_{27}FN_2O_5HCl$: C 65.15, H 6.15, N 6.33, found: C 64.95, H 5.98, N 6.21.

Bis(tosyloxy)methane: A solution of silver *p*-toluenesulfonate (0.05 mol) and methyl iodide (0.023 mol) in acetonitrile (50 mL) was heated at reflux for 24 h. The mixture was filtered, and the volatile solvent was removed under reduced pressure. The solid product was dissolved in warm 1,2-dichloroethane (150 mL) and then filtered to remove the excess amount of silver methanesulfonate. The solvent was removed by distillation to give a solid that was recrystallized (absolute ethanol). Yield: 87%; mp: 116–117 °C; MS (ESI$^+$): *m/z*: 379 [*M* + Na]$^+$; MS–MS (ESI$^+$): *m/z* (%): 349 (100), 155 (2).

Methylene fluorotosylate: A solution of tetrabutylammonium fluoride (1.1 mmol in 2 mL acetonitrile) was added to a solution of bis(tosyloxy)methane (1 mmol) in dry acetonitrile (10 mL), and the mixture was stirred at reflux. After 2 h, the solvent was removed under reduced pressure, and the residue was dissolved in EtOAc (30 mL) and washed with H_2O (30 mL). The organic solution was dried ($MgSO_4$), filtered, and concentrated under reduced pressure. The residue was purified by column chromatography (hexane/EtOAc = 5:2). Yield: 31%. GC–MS: *m/z* (%): 204 (28) [*M*]$^+$, 155 (49), 91 (100).

2-[2-(2-Fluoromethyl-5-methoxyphenyl)oxazol-4-ylmethyl]-6,7-dimethoxy-1,2,3,4-tetrahydroisoquinoline (6): A suspension of NaH (60%, mmol) in dry DMF (3 mL) was stirred at RT for 10 min. A solution of phenol **12** (1 mmol) in DMF (1 mL) was added, and the mixture was stirred for 1 h. A solution of 2-fluoromethyl tosylate (1.1 mmol) in DMF (1 mL) was added, and the mixture was stirred for 24 h. H_2O was added until effervescence ceased. The solvent was evaporated, and the residue was partitioned between H_2O (20 mL) and $CHCl_3$ (20 mL). The organic phase was separated, and the aqueous phase was extracted with $CHCl_3$ (3 × 50 mL). The combined organic layer was dried (Na_2SO_4) and concentrated. The residue was purified on silica gel column chromatography ($CHCl_3$/MeOH = 19:1). Yield: 2%; MS (ESI$^+$): *m/z*: 451 [*M* + Na]$^+$; MS–MS (ESI+): *m/z* (%): 431 (4), 409 (100).

Radiolabeled chemistry

[^{11}C]-1: [^{11}C]-**1** was produced from desmethyl-**1** as previously described.[27] The radiochemical yield was ≥60% end of bombardment (EOB) based on [^{11}C]methyl triflate), radiochemical purity ≥99%, and the specific activity ≥100 GBq μmol^{-1}.

[^{11}C]-5: [^{11}C]Methyl iodide was added to a solution of DMSO (300 μL) containing precursor **12** (1 mg, 2.2 μmol) and KOH (14 mg). After trapping [^{11}C]methyl iodide, the temperature was raised to 125 °C for 1 min, and after this time the mixture was quenched with 1 M HCl (1 mL). The mixture was purified and formulated as reported in the section General Procedures. The radiochemical yield was ≥40% (EOB based on [^{11}C]methyl iodide), radiochemical purity ≥99%, and the specific activity ≥100 GBq μmol^{-1} (EOB values).

Drying procedure for [^{18}F]fluoride: Aqueous [^{18}F]fluoride was produced by the ^{18}O (p,n)^{18}F nuclear reaction by irradiation of [^{18}O]water with a Scanditronix MC-17 cyclotron. The [^{18}F]fluoride solution was passed through an activated Sep-Pak Light Accell plus QMA anion-exchange cartridge (Waters) to recover [^{18}O]water. [^{18}F]fluoride was eluted from the cartridge with K_2CO_3 (5 mg mL^{-1}, 1 mL) and was collected in a vial containing Kryptofix 2.2.2 (15 mg). Acetonitrile (dried on molecular sieves, 1 mL) was added to this solution, and the solvents were evaporated at 130 °C. The [^{18}F]KF/Kryptofix complex was dried three times by the addition of acetonitrile (0.5 mL), followed by evaporation of the solvent.

[^{18}F]Fluoromethyl triflate: The synthesis of [^{18}F]bromofluoromethane was performed in an automated synthesis apparatus (Fluoro Methylation Unit, model FMU-101, Veenstra) A solution of dibromomethane (500 μL) in acetonitrile (700 μL) was added to the dry [^{18}F]KF/Kryptofix complex. The mixture was heated at 115 °C for 5 min, and after the reaction, formed [^{18}F]CH_2BrF was passed through four Sep-Pak silica cartridges connected in series by He flow (100 mL min^{-1}) to separate the product from CH_2Br_2. Once [^{18}F]CH_2BrF started to elute from the Sep-Pak, it was allowed to flow through the heated (190 °C) AgOTf column to convert it into [^{18}F]fluoromethyl triflate (decay-corrected radiochemical yield from [^{18}F]fluoride was 35–40%). [^{18}F]Fluoromethyl triflate was trapped at 0 °C in a second reaction vessel containing the precursor for the synthesis of [^{18}F]-**6**.

[^{18}F]-6: Precursor **12** (0.5 mg) was treated with NaH (5 mg) in dry DMF (0.2 mL). [^{18}F]Fluoromethyl triflate was trapped in this solution at 0 °C. After trapping of [^{18}F]fluoromethyl triflate, the reaction vessel was heated at 125 °C for 10 min, and after cooling, the mixture was diluted to 1 mL with 0.1 mol L^{-1} acetonitrile/sodium acetate and filtered with HV filter (0.45 μm). The product was purified and formulated as reported in the General Procedures. The radiola-

beled compound was obtained in 3–10% radiochemical yield from [^{18}F]fluoride (decay corrected) in 80–90 min. The specific activity of [^{18}F]-**6** was $\geq$50 GBq μmol^{-1} and the radiochemical purity was 95% (EOS values)

[^{18}F]Fluoroethyl tosylate: A solution of ethyleneglycol-1,2-ditosylate (5 mg) in dry acetonitrile (0.5 mL) was added to the dried [^{18}F]KF/Kryptofix complex, and the mixture was heated at 125 °C for 5 min. The product was purified by dissolving the product in DMF (0.3 mL) and passing through a Sep-Pak Alumina N cartridge. Kryptofix, K_2CO_3, and the excess amount of [^{18}F]fluoride were retained on the cartridge, and the product was eluted with DMF (0.3 mL). The procedure required approximately 50 min from [^{18}F]fluoride, decay corrected, and it provided [^{18}F]fluoroethyl tosylate with an overall radiochemical yield of 20 to 40%.

[^{18}F]-7: Precursor **12** (0.5 mg) and NaH (3–4 mg) dissolved in DMF (0.5 mL) were added to a solution of [^{18}F]fluoroethyl tosylate in DMF (0.5 mL). The mixture was heated for 15 min at 125 °C and after cooling down was diluted to 0.1 mol L^{-1} acetonitrile/sodium acetate (1 mL) and then filtered through a HV filter (0.45 μm). The product was purified and formulated as reported in the General Procedures. The radiolabeled compound was obtained in 3–10% radiochemical yield from [^{18}F]fluoride (decay corrected) in 80–90 min. The specific activity of [^{18}F]-**7** was $\geq$100 GBq μmol^{-1} and the radiochemical purity was 95% (EOS values)

Biological methods

In vitro experiments of nonradioactive 5 and 7

Permeability experiments: Caco-2 cells were seeded onto a Millicell assay system (Millipore), for which a cell monolayer was set in between a filter cell (apical) and a receiver plate (basolateral) at a density of 10000 cells per well. The culture medium was replaced every 48 h, and the cells were kept in culture for 21 days. The trans epithelial electrical resistance (TEER) of the monolayers was measured daily, before and after the experiment, by using an epithelial volt–ohm meter (Millicell-ERS). Generally, TEER values greater than 1000× for a 21 day culture were considered optimal. Apical to basolateral (P_{app}, A→B) and basolateral to apical (P_{app}, B→A) permeability of the drug were measured at 120 min and at various drug concentrations (1–100 μM). After 21 days of Caco-2 cell growth, the medium was removed from the filter wells and from the receiver plate, which were filled with fresh Hank's balanced salt solution (HBSS) buffer (Invitrogen). This procedure was repeated twice, and the plates were incubated at 37 °C for 30 min. After incubation time, the HBSS buffer was removed and compounds were added to the filter well at various concentrations (1–100 μM), whereas fresh HBSS was added to the receiver plate. The plates were incubated at 37 °C for 120 min. Afterward, samples were removed from the apical (filter well) and basolateral (receiver plate) side of the monolayer to measure the permeability. The apparent permeability (P_{app}) was calculated by using Equation (1):

$$P_{app}\ [\mathrm{nm\,s^{-1}}] = \left(\frac{V_A}{area \times time}\right) \times \left(\frac{[drug]_{acceptor}}{[drug]_{initial}}\right) \quad (1)$$

in which V_A is the volume in milliliters in the acceptor well, *area* is the surface area of the membrane (0.11 cm^2 of the well), *time* is the total transport time in seconds (7200 s), $[drug]_{acceptor}$ is the concentration of the drug measured by UV spectroscopy, and $[drug]_{initial}$ is the initial drug concentration (1×10^{-4} M) in the apical or basolateral wells.

Calcein-AM experiment: These experiments were performed as described by Feng et al.[29] and Rautio et al.[30] with minor modifications. Madin–Darby canine kidney (MDCK) cells overexpressing each transporter (i.e., MDCK-MDR1, MDCK-BCRP, and MDCK-MRP1) were grown in DMEM high glucose supplemented with 10% fetal bovine serum, 2 mM glutamine, 100 U mL^{-1} penicillin, and 100 g mL^{-1} streptomycin in a humidified incubator at 37 °C under a 5% CO_2 atmosphere. Each cell line (50000 cells per well) was seeded into black CulturePlate 96-well plate with medium (100 μL) and allowed to become confluent overnight. Each compound (100 μL) at various concentrations (1–100 μM) was solubilized in culture medium and was added to the monolayers. The 96-well plate was incubated at 37 °C for 30 min. Calcein-AM was added in of phosphate-buffered saline (PBS, 100 μL) to yield a final concentration of 2.5 μM, and the plate was incubated for 30 min. Each well was washed with ice-cold PBS (3×). Saline buffer was added to each well, and the plate was read by a Victor 3 plate reader (PerkinElmer) at excitation and emission wavelengths of 485 and 535 nm, respectively. Under these experimental conditions, Calcein cell accumulation in the absence and in the presence of the tested compound was evaluated and the fluorescence basal level was estimated by untreated cells. In treated wells, the increase in fluorescence with respect to the basal level was measured. EC_{50} values were determined by fitting the fluorescence increase percentage versus log [dose].

ATPlite assay: The MDCK-MDR1 cells were seeded into a 96-well microplate in complete medium (100 μL) at a density of 2×10^4 cells per well.[31] The plate was incubated overnight under a humidified atmosphere of 5% CO_2 at 37 °C. The medium was removed and complete medium (100 μL) in the presence or absence of different concentrations (1–100 μM) of each compound was added. The plate was incubated for 2 h under a humidified atmosphere of 5% CO_2 at 37 °C. Mammalian cell lysis solution (50 μL) was added to all wells, and the plate was shook for 5 min in an orbital shaker. Substrate solution (50 μL) from the assay kit was added to all wells, and the plate was shook for 5 min in an orbital shaker. The plate was adapted in the dark for 10 min and the luminescence was measured.

Metabolism experiment in microsomes: Human liver microsomes were purchased from BD Biosciences (Woburn, MA), NADPH was purchased by Sigma–Aldrich. The experiment was performed following the protocol available on the website of BD Biosciences (www.bdbiosciences.com). Tested compounds (14 μL of 4 mM solution in DMSO) were incubated with 20 mg mL^{-1} human liver microsomal proteins (70 μL) in PBS (2.6 mL) at 37 °C for 5 min. NADPH solution (20 mM) was freshly made in PBS and was added (140 μL) to the tubes in final concentration of 1 mM to start the reaction. The first sample (400 μL) was taken immediately, and the reaction was stopped by the addition of acetonitrile + 0.1% formic acid (800 μL). Other samples were taken at time points of 15, 30, 45, 60, 90, and 120 min. Three control tubes were also incubated for 120 min: one without microsomes, one without NADPH, and one without test compound. In these tubes, volume was replaced by PBS. Sample tubes were vortexed and centrifuged for 6 min at 12000 rpm. Samples were injected into the UPLC–MS–MS (Waters Xevo QTOF MS, column ACQUITY UPLC BEH C18 1.7 μm, eluent H_2O/CH_3CN + 0.1% HCOOH, flow 0.6 mL min^{-1}, ESI positive mode). The Metabolynx XS software (Waters) was used for the analysis of metabolites.

In vitro experiments of [^{11}C]-5, [^{18}F]-7, and [^{18}F]-6

Separation of subcellular fractions for detecting fraction-specific tracer uptake/binding: The following procedure was modified from the original subcellular fractionation protocol available on the website of Abcam (www.abcam.com). At the time of use: 10 mL (depending on the number of samples) of the subcellular fraction buffer were taken and 1 mM DTT (50 μL) and protease inhibitor cocktail (50 μL) were added. After pre-incubation and incubation with the above-mentioned modulators and/or ATP, the media containing the radiotracer was removed from the cells. Three to four samples of these radioactive media were transferred into clean prelabeled Eppendorf tubes to use as an injected-dose (ID) correction. The remaining cells in the plate were harvested by trypsinization and were collected into clean Eppendorf tubes containing media (without serum) to neutralize the trypsin. This cell suspension was readily centrifuged at 6000×g for 2 min to obtain the cell pellet. After removing all the supernatant, the cold subcellular fraction buffer (500 μL) was added to each cell pellet. Using distinct 25G needles and 1 mL syringes to avoid cross contamination, the cell pellets were homogenized 10 times for each sample. Until all tubes were homogenized, the tubes were kept on ice. After homogenization, another set up of centrifugation at 500×g for 5 min was performed. The supernatants (cytoplasmic extract) were then immediately transferred into clean prelabeled tubes on ice and kept until gamma counting. To the remaining pellet, more of the cold subcellular fraction buffer (500 μL) was added, and it was vortexed for 5 s on the highest setting and kept on ice. After all tubes were vortexed, another centrifugation set up of 3000×g for 5 min was performed. The supernatants (membrane extract) were then transferred into clean prelabeled tubes on ice. The remaining pellet, which was called the "rest of the cells", was also counting in the gamma counter.

Transport assay using the radiolabeled compounds: Complete RPMI medium including L-glutamine and FCS (fetal calf serum) were used throughout. Cells were seeded on microporous polycarbonate membrane filters (8.0 μm pore size, 6.5 mm diameter, Transwell 3422, Costar Corp., Cambridge, MD) at a density of 3×10^4 cells per well. The cells were grown for 3 days (72 h) in complete medium with one medium replacement. At 1–2 h before the start of the experiment, medium at both the apical and the basal side of the monolayer was replaced with a total of 700 μL (100 μL in the apical and 600 μL in the basal side) of complete medium. The experiment was started by adding P-gp modulator **3**,[30] **1**, or **13** (stock solution of 10 mM) in the apical side of the cell layer for 30 min and was followed by the addition of the radiotracer (15 μL, 6.6 kBq μL^{-1}), which was incubated for more 30 min at 37 °C under an atmosphere of 5% CO_2 with regulated humidity. No P-gp modulator was added in the controls (only the radiolabeled compound). After the incubating period, all media from each compartment was removed and transferred to clean Eppendorf tubes for subsequent radioactivity measures in the gamma counter. The percentage of the injected dose (%ID) was then calculated.

Acknowledgements

The UPLC–MS-QTOF facility is supported financially by The Netherlands Organisation for Health Research and Development (ZonMw) project number: 91111007. We thank Bram Maas for his assistance with the radiochemistry.

Keywords: glycoproteins · inhibitors · isotope labeling · positron emission tomography · radioligands

[1] P. Kannan, C. John, S. S. Zoghbi, C. Haldldin, M. M. Gottesman, R. Gottesman, B. Innis, M. D. Hall, *Clin. Pharmacol. Ther.* **2009**, *86*, 368–377.
[2] C. L. Graff, G. M. Pollack, *Curr. Drug Metab.* **2004**, *5*, 95–108.
[3] J. R. Cirrito, R. Deane, A. M. Fagan, M. L. Spinner, M. Parsadanian, M. B. Finn, H. Jiang, J. L. Prior, A. Sagare, K. R. Bales, S. M. Paul, B. V. Zlokovic, D. Piwnica-Worms, D. M. Holtzman, *J. Clin. Invest.* **2005**, *115*, 3285–3290.
[4] A. L. Bartels, *Curr. Pharm. Des.* **2011**, *17*, 2771–2777.
[5] A. H. Abuznait, A. Kaddoumi, *Chem. Neurosci.* **2012**, *3*, 820–831.
[6] A. Elali, S. Rivest, *Front. Physiol.* **2013**, *13*, 1–6.
[7] C. Kuntner, J. P. Bankstahl, M. Bankstahl, J. Stanek, T. Wanek, G. Stundner, R. Karch, R. Brauner, M. Meier, X. Ding, M. Müller, W. Löscher, O. Langer, *Eur. J. Nucl. Med. Mol.* **2010**, *37*, 942–953.
[8] M. Bauer, M. Zeitlinger, R. Karch, P. Matzneller, J. Stanek, W. Jäger, M. Böhmdorfer, W. Wadsak, M. Mitterhauser, J. P. Bankstahl, W. Löscher, M. Koepp, C. Kuntner, M. Müller, O. Langer, *Clin. Pharmacol. Ther.* **2012**, *91*, 227–233.
[9] a) A. L. Bartels, O. L. de Klerk, R. Kortekaas, J. J. de Vries, K. L. Leenders, *Curr. Top. Med. Chem.* **2010**, *10*, 1775–1784; b) W. C. Kreisl, J. Liow, S. N. Kimura, N. Seneca, S. S. Zoghbi, C. L. Morse, P. Herscovitch, V. W. Pike, R. B. Innis, *J. Nucl. Med.* **2010**, *51*, 559–566.
[10] M. Lubberink, G. Luurtsema, B. N. van Berckel, R. Boellaard, R. Toornvliet, A. D. Windhorst, E. J. Franssen, A. A. Lammertsma, *J. Cereb. Blood Flow Metab.* **2007**, *27*, 424–433.
[11] G. Luurtsema, C. F. Molthoff, R. C. Schuit, A. D. Windhorst, A. A. Lammertsma, E. J. Franssen, *Nucl. Med. Biol.* **2005**, *32*, 87–93.
[12] H. Nakanishi, A. Yonezawa, K. Matsubara, I. Yano, *Eur. J. Pharmacol.* **2013**, *710*, 20–28.
[13] T. Wanek, S. Mairinger, O. Langer, *J. Labelled Compd. Radiopharm.* **2013**, *56*, 68–77.
[14] G. Luurtsema, R. C. Schuit, R. P. Klok, J. Verbeek, J. E. Leysen, A. A. Lammertsma, A. D. Windhorst, *Nucl. Med. Biol.* **2009**, *36*, 643–649.
[15] P. Kannan, S. Telu, S. Shukla, S. V. Ambudkar, V. W. Pike, C. Halldin, M. M. Gottesman, R. B. Innis, M. D. Hall, *ACS Chem. Neurosci.* **2011**, *2*, 82–89.
[16] N. A. Colabufo, A. van Waarde, *Curr. Top. Med. Chem.* **2010**, *10*, 1701–1702.
[17] S. Mairinger, T. Wanek, C. Kuntner, Y. Doenmez, S. Strommer, J. Stanek, E. Capparelli, P. Chiba, M. Müller, N. A. Colabufo, O. Langer, *Nucl. Med. Biol.* **2012**, *39*, 1219–1225.
[18] A. van Waarde, N. K. Ramakrishnan, A. A. Rybczynska, P. H. Elsinga, F. Berardi, J. R. de Jong, C. Kwizera, R. Perrone, M. Cantore, J. W. Sijbesma, R. A. Dierckx, N. A. Colabufo, *J. Med. Chem.* **2009**, *52*, 4524–4532.
[19] N. Tournier, H. Valette, M. A. Peyronneau, W. Saba, S. Goutal, B. Kuhnast, F. Dollé, J. M. Scherrmann, S. Cisternino, M. Bottlaender, *J. Nucl. Med.* **2011**, *52*, 415–423.
[20] S. D. Bruyne, L. Wyffels, L. Moerman, J. Sambre, N. A. Colabufo, F. Berardi, R. Perrone, F. D. Vos, *Bioorg. Med. Chem.* **2010**, *18*, 6489–6495.
[21] N. A. Colabufo, F. Berardi, M. G. Perrone, E. Capparelli, M. Cantore, C. Inglese, R. Perrone, *Curr. Top. Med. Chem.* **2010**, *10*, 1703–1714.
[22] R. B. Wang, C. L. Kuo, L. L. Lien, E. J. Lien, *J. Clin. Pharm. Ther.* **2003**, *28*, 203–228.
[23] J. W. Polli, S. A. Wring, J. E. Humphreys, L. Huang, J. B. Morgan, L. O. Webster, C. S. Serabjit-Singh, *J. Pharmacol. Exp. Ther.* **2001**, *299*, 620–638.
[24] N. A. Colabufo, F. Berardi, M. G. Perrone, M. Cantore, M. Contino, C. Inglese, M. Niso, R. Perrone, *ChemMedChem* **2009**, *4*, 188–195.
[25] A. Calcabrini, J. M. García-Martínez, L. González, M. J. Tendero, M. T. Ortuño, P. Crateri, A. Lopez-Rivas, G. Arancia, P. González-Porqué, J. Martín-Pérez, *Carcinogenesis* **2006**, *27*, 1699–1712.
[26] N. A. Colabufo, F. Berardi, M. Cantore, M. G. Perrone, M. Contino, C. Inglese, M. Niso, R. Perrone, A. Azzariti, G. M. Simone, L. Porcelli, A. Paradiso, *Bioorg. Med. Chem.* **2008**, *16*, 362–373.
[27] D. M. Jewett, *Appl. Radiat. Isot.* **1992**, *43*, 1383–1385.
[28] T. D. Wegman, B. Maas, P. H. Elsinga, W. Vaalburg, *Appl. Radiat. Isot.* **2002**, *57*, 505–507.

[29] a) B. Feng, J. B. Mills, R. E. Davidson, R. J. Mireles, J. S. Janiszewski, M. D. Troutman, S. M. De Morais, *Drug Metab. Dispos.* **2008**, *36*, 268 – 275; b) O. A. Fahmi, T. S. Mauer, M. Kish, E. Cardenas, S. Boldt, D. Nettleton, *Drug Metab. Dispos.* **2008**, *36*, 1698 – 1708.

[30] J. Rautio, J. E. Humphreys, L. O. Webster, A. Balakrishnan, J. P. Keogh, J. R. Kunta, C. J. Serabjit-Singh, J. W. Polli, *Drug Metab. Dispos.* **2006**, *34*, 786 – 792.

[31] A. L. Kangas, L. Groenroos, M. Nieminen, *Med. Biol.* **1984**, *62*, 338 – 343.

Received: September 14, 2015
Revised: October 19, 2015
Published online on November 13, 2015